Journal of Chromatography A, 1218 (2011) 3255–3261

Contents lists available at ScienceDirect

Journal of Chromatography A

journal homepage: www.elsevier.com/locate/chroma

Description of the response of a fiber optic velocity sensor applied to capillary gas chromatography

Serge Caron*, Claude Paré, Patrick Paradis, Antoine Proulx

Institut national d'optique, 2740 rue Einstein, Québec, Québec, Canada G1P 4S4

ARTICLE INFO

Article history:
Available online 7 April 2011

Keywords:
Fiber optics chemical sensor
Capillary gas chromatography
Migration rate sensor
Sensor linearity
Gas diffusion
Polarimetric interferometry
Gas chromatography detector

ABSTRACT

This paper explores the response of a novel fiber optics sensor allowing real-time determination of the migration rate of vapor zones in capillary gas chromatography. The sensitivity is related to the gradient of the vapor zone distribution in the capillary and it is highest when vapor zones show steep variations in concentration. The expected linearity between the height of the velocity peaks and the response of a thermal conductivity detector is demonstrated experimentally. The sensor can be used to infer an approximate value of the analyte diffusion coefficient from the time response. Finally, the time evolution of the envelope of the optical signal is explained with experimental evidences.

1. Introduction

In this paper, we present results of a theoretical modeling of the mode coupling mechanism that forms the basis of the operational principle of the migration velocity sensor that was presented earlier [1]. The sensor, initially developed for capillary gas chromatography (GC), is a distributed fiber optic sensor that measures the velocity of vapors zones in real time, as they migrate inside the capillary.

Using optical sensors as detectors in GC is not new. For instance, Liu et al. [2] have proposed the use of a Fabry–Perot interferometer inserted in a hole drilled on the side of a capillary. Previously, other researchers have studied the use of optical ring resonators as a detector, permitting the detection of nanograms of analytes [3]. Another fiber optic detector based on mode-filtering has also been studied by Synovec et al. [4,5]. All of these fiber optic sensors are not distributed sensors, and once decoded, the information provided by these detectors is not much different from those of other detectors used in GC: they measure the amount of analyte passing in the detector over time. The polarimetric sensor that we developed [1,6–10] differs from the previous ones in that it is really a *distributed sensor*. Light is injected at the entrance of the capillary fiber, propagates along the entire length of the capillary, where it interacts with the analyte present in the column, and is then detected at the capillary output. Decoding the optical signal gives information on what is happening *inside* the capillary in real time. It is worth noting that the distributed measurement does not give the position of the vapor zones, but their velocities. The processed signal given by this velocity sensor translates into a series of peaks whose positions correspond to the migration rate of the vapor zones.

The sensor uses a birefringent optical fiber in which is located a capillary that runs along its length. This capillary makes an angle of 30° relatively to the elliptical core of the embedded waveguide. Hereafter, this optical fiber will be referred to as the capillary fiber. The operating principle of the sensor, which is polarization modes coupling caused by a rotation of birefringence axes induced by vapor absorption in the stationary phase, and the first results of velocities measurement, permitting the identification of the analytes, have been published recently [1]. The present paper is instead focused on the *quantitative* aspect of the sensor's signal. To this end, we developed a mathematical model of the mode coupling mechanism that describes the amplitude of the optical signal in relation to the amount of analyte migrating in the capillary. We apply this model to a Gaussian distribution of the vapor zone in order to highlight the characteristics of the sensor. Experimental results on the linearity of the sensor and the effect of zone spreading are also presented. Finally, the phenomenon of the signal baseline variation (envelope) presented in the previous paper is now explained by a simple model with experimental support.

2. Description of the sensor optical signal

A close look at a typical optical signal measured during the passage of a single analyte in the capillary fiber will help to introduce

* Corresponding author. Tel.: +1 418 657 7006; fax: +1 418 657 7009.
E-mail address: serge.caron@ino.ca (S. Caron).

0021-9673/$ – see front matter © 2011 Elsevier B.V. All rights reserved.
doi:10.1016/j.chroma.2011.03.029

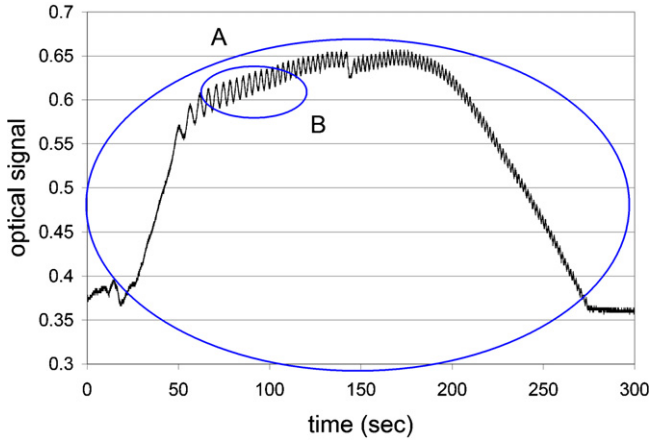

Fig. 1. Example of an optical signal recorded during the displacement of a vapor zone in the capillary fiber. Injection of 1 μL of cyclopentane with a split of 200. The column temperature was 30 °C.

the analysis. Fig. 1 below shows an experimental measurement following the injection of cyclopentane. The signal can be separated into two parts, whose features are attributable to two different optical mechanisms. Part A is an increase of the signal baseline (the average transmitted optical power) which disappears when the analyte leaves the capillary fiber. In Fig. 1, this increase is very significant as it corresponds to 75% of the basic signal. This part of the signal will be explained in Section 5. Part B of the signal is a rapid oscillation corresponding to polarization modes coupling along the capillary optical fiber. This is the part of the signal that is of interest as it enables the measurement of the migration rate. The oscillation frequency is proportional to the moving velocity of the cyclopentane vapor zone. Fig. 1 shows that this frequency increases with time, because the vapor zone accelerates, due to a decompression of the helium carrier gas [1]. One can also observe that the amplitude of the oscillation decreases with time, from about 7% of the average signal at the beginning to less than 1% at the end. It is the relationship between this amplitude and the vapor concentration and with the form of the vapor zone as well that will be established in the first place.

A temporal Fourier transform applied on a selected portion of the signal gives a velocity peak whose position (related to the oscillation frequency) determines the velocity of the vapor zone and whose height (related to the amplitude of oscillation) is related to the quantity in the vapor zone. An example of such a peak calculated from the signal of Fig. 1 in the 80–100 s region is shown in Fig. 2. In our previous studies [1], the emphasis was mostly on the position of the velocity peak, on the abscissa; here, the focus will be on the height of this peak, on the ordinate.

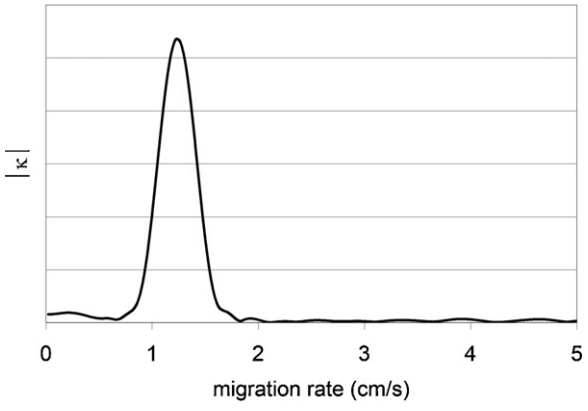

Fig. 2. The migration rate peak calculated from the signal in Fig. 1 (interval between 80 and 100 s).

3. Experimental

All experiments presented here were performed in exactly the same conditions as those reported in the previous paper [1]. The capillary optical fiber had an inner diameter of 100 μm with a 0.5 μm thick poly(dimethylsiloxane) stationary phase. Its beat length was 3.9 cm at a wavelength of 1550 nm. The capillary fiber length was 450 cm and it was connected to a Varian CP-3800 Gas Chromatograph through two short uncoated pre-columns, 63.9 and 77.5 cm long. The carrier gas was helium; its inlet pressure was 412 kPa. The chromatograph was operated at 30 °C. Both split–splitless injector and thermal conductivity detector (TCD) were operated at 250 °C. The TCD filament was heated at 300 °C and it was set at its optimal sensitivity (range 0.05). The TCD was selected because it has the most similar sensitivity to that of the optical sensor.

Nothing was done to optimize the chromatographic performance. GC conditions were set-up quite arbitrarily for optical measurements only. Our main goal was to demonstrate the linearity between the optical sensor and the thermal conductivity detector and the time dependence of the modulation amplitude.

Optical measurements were done using an Agilent 8164B Lightwave Measurement System.

4. Description of the oscillation of the optical signal

The first model of the polarimetric sensor associated the vapor zone to a birefringent plate tilted at an angle φ [7] and calculations were done using Jones matrices [11]. The model gives the variation of the intensity of the light transmitted by the sensor (the signal) during the migration of a vapor zone at a velocity v. The resulting equation reads as:

$$I(t) = \frac{I_0}{2}\{1 - |\kappa|\cos[\Delta\beta(L - vt) + \theta]\}, \quad (1)$$

where I_0 is the light intensity at the entrance of the capillary fiber; $|\kappa|$ is the modulus of the amplitude of oscillation (κ can be a complex number); L is the length of the capillary fiber; v is the velocity of the vapor zone, here assumed as constant for simplification; t represents the time and θ, a phase term that can be omitted as it disappears after Fourier transformation. The application of this Fourier transform gives a spectrum showing peaks whose central position corresponds to the speed v of the vapor zone at a given time. Finally, $\Delta\beta$, is the difference in the propagation constants of both x and y polarized waves:

$$\Delta\beta = \frac{2\pi}{\lambda}B = \frac{2\pi}{L_b} = \frac{2\pi}{\lambda}(n_y - n_x). \quad (2)$$

L_b is the beat length of our fiber and is equal to 3.9 cm at the working wavelength λ of 1550 nm [1]; the value of $\Delta\beta$ is thus 1.61 cm^{-1}.

Eq. (1) is sufficient to properly describe the zones vapor velocities. This has been demonstrated experimentally [1].

4.1. Relationship between the amplitude $|\kappa|$ and the vapor zone distribution

The model of polarization mode coupling shows that the rotation of the polarization axes, caused by the refractive index change of the stationary phase, is small in the vapor zone. For instance, numerical simulations have shown that the rotation is around 8° for a refractive index change of 0.12 (the difference between water and silica) [7]. Moreover, the refractive index change caused by the concentration of the analyte absorbed in the stationary phase will

be much smaller; it cannot be higher than few percents of the difference between the refractive index of the stationary phase itself and the one of the analyte. Consequently we can assume that the rotation of the polarization axes according to the concentration of analyte is always small and, to first order of perturbation, is linear.

To complete the description of the optical signal, the amplitude of oscillation κ (the mode coupling strength) must be related to the vapor zone distribution. A detailed mathematical modeling of the polarization mode coupling mechanism underlying the evolution of the optical signal will be presented elsewhere [12]. For the present purpose, it is sufficient to present the main result. It comes out of this theoretical work that the amplitude κ is proportional to the gradient of the vapor zone distribution. We found:

$$\kappa = \kappa(\Delta\beta) = A \int_0^L \left(\frac{dC(z)}{dz}\right) e^{-i\Delta\beta z} dz, \quad (3)$$

where A is a factor of proportionality, $C(z)$ describes the spatial variation of the analyte concentration in the stationary phase along the capillary of length L and $i = \sqrt{-1}$. The equation shows that the value of κ will change with the time evolution of the vapor zone distribution $C(z)$. It suggests that a vapor zone showing steep variations in concentration will give rise to a *larger amplitude* of oscillation. This is consistent with the theory of birefringent fibers according to which mode coupling is more pronounced when it occurs in a much localized zone.

When the vapor zone is located entirely within the capillary fiber (i.e.: it has fully entered into the column but has not begun to exit), one can extend the limits of integration to $\pm\infty$ and Eq. (3) then reads as a Fourier transform performed over space z:

$$\kappa(\Delta\beta) = A \int_{-\infty}^{\infty} \left(\frac{dC(z)}{dz}\right) e^{-i\Delta\beta z} dz, \quad (4)$$

(This Fourier transform should not be confused with the Fourier transform of the signal described by Eq. (1), which is performed over time t). Using the derivative theorem ([13], p. 122), the amplitude κ can be directly linked to the distribution of the vapor zone $C(z)$:

$$\kappa(\Delta\beta) = A\,FT\left(\frac{dC(z)}{dz}\right) = A(i\Delta\beta)FT(C(z)), \quad (5)$$

where *FT* means Fourier transform.

4.2. Application to a Gaussian distribution

Hereafter, the particular case of a vapor zone with a Gaussian distribution is considered. The Gaussian distribution is the solution for both the model of plates using random walk and binomial distribution, and the equilibrium model, using equations of diffusion and mass balance. It is of course an ideal case.

The normalized concentration of vapor absorbed in the stationary phase is given by the following expression ([14], p. 50):

$$C(z,t) = \frac{N}{\sqrt{4\pi D_{eff} t}} \exp\left\{-\frac{(z-vt)^2}{4D_{eff} t}\right\}. \quad (6)$$

Here D_{eff} is an *effective* diffusion coefficient and the value of $2D_{eff}t$ is equal to the variance σ^2 of the Gaussian distribution. In this equation, a pre-exponential factor N has been added. N is the amount of analyte per unit area of the stationary phase cross section and it is proportional to the total amount of analytes in the capillary through the partition coefficient. The application of Eq. (5) gives:

$$\left|\kappa(\Delta\beta)\right| = A\,N\,\Delta\beta \exp\{-D_{eff} t \Delta\beta^2\}. \quad (7)$$

Eq. (7) is an approximation of reality as it is based on the ideal case of a Gaussian distribution; however, as demonstrated below by the experimental results, it correctly predicts an exponential decrease of the amplitude over time. Eq. (7) also indicates that the signal amplitude is proportional to the amount N of analyte in the stationary phase. (More generally, as will be discussed elsewhere, inspection of Eq. (4) and of the diffusion equation that governs the spatio-temporal evolution of the vapor distribution, suggests that the linear proportionality between κ and N is general, i.e. it does not depend on the Gaussian approximation. This is true, however, as long as the vapor injection is controlled so as to make the evolution of the *shape* of the distribution independent of the injected quantity.)

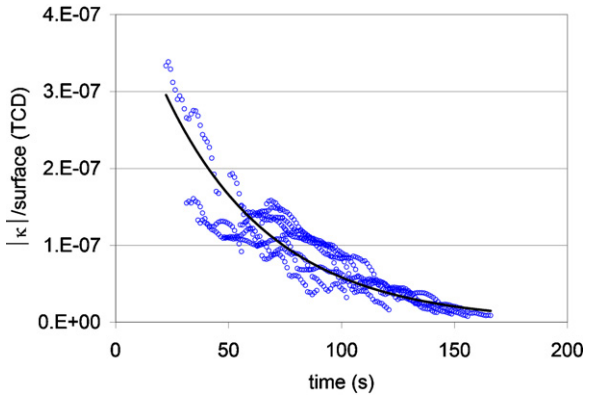

Fig. 3. $|\kappa|$ according to time, normalized to the peak surface measured with the TCD at the column output. The solid line is an exponential best fit.

4.3. Experimental demonstration of sensor's linearity

How can one perform a quantitative analysis when, as Eq. (7) suggests, the height of the velocity peak decreases with time? This problem of the time dependence of $|\kappa|$ can be solved by performing a least squares regression ([15], p. 188 and following) on the $|\kappa|$ temporal curve. An experimental example is shown in Figs. 3 and 4. Least squares regression was performed as follows. Firstly, the curves $|\kappa|$ were normalized to the area of the elution peaks measured by the TCD detector (Fig. 3) and a best fit with an exponential function was calculated. The amount C of pentane detected by the optical sensor was then calculated by a regression with this best fit (the equation is given in Appendix A).

The units of C are the same unit area as measured by the TCD because these values were used for normalization.

Fig. 4 below confirms that the relation between the velocity sensor and the TCD is linear, except for the largest amounts of pentane injected. The deviation from linearity occurs when the injected quantities are equal to or greater than 3 μl (with a split of 200) in the 100 μm capillary. Making abstraction of sensitivity, we believe that the linearity observed in Fig. 4 over the first half of the tested range in injected quantity is sufficient to conclude to the real poten-

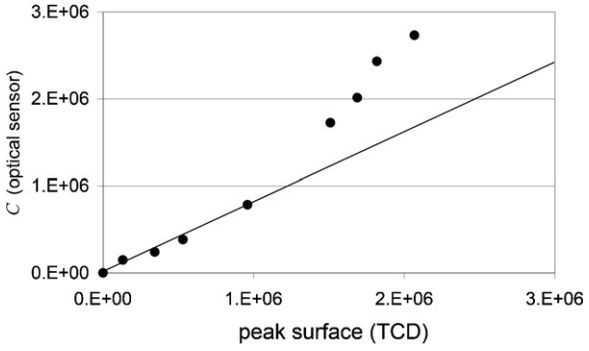

Fig. 4. Relation between the signal of the optical velocity sensor and the signal from the TCD.

tial of the sensor for quantitative analysis, although at present, the dynamic range of the sensor remains to be clarified.

For highest injected amounts, differences in the form of the injected peaks most probably explain the deviation from the linear relationship between height of the velocity peaks and TCD surface. Another contribution for this deviation can come from a variation of the birefringence B and hence $\Delta\beta$ (see Eq. (2)); indeed Eq. (7) predicts that a change of its value will change the amplitude $|\kappa|$. The possible nonlinear partition of the analyte between mobile and stationary phases as the injected amounts are very large could also give rise to a nonlinear behavior.

Fig. 3 shows a significant spreading of the experimental results. Part of this can be attributed to the limited control of the injection. As discussed above, a change of the initial conditions (temporal variation of the flow) at the injection implies a variation of the evolution (diffusion) of the vapor zone in the capillary, hence modifying the optical signal, as suggested by Eq. (3).

4.4. Zone spreading and the coefficient of diffusion

The approximation of Eq. (7) implies that a plot of $|\kappa|$ versus time should allow the determination of the effective diffusion coefficient D_{eff} of the analyte in the carrier gas. (Reminding that Eq. (7) is an approximation, one should not expect to get an accurate value.)

With reference to Jönsson [14], the coefficient of diffusion of the vapor is given by:

$$D = \frac{D_{eff}}{p}, \tag{8}$$

where p is the retention ratio [16]. This value is calculated by dividing the hold-up time t_M (measured with CH_4) by the retention time t_R of the analyte. Here it is assumed that the value of D is equal to the value of the coefficient of diffusion of the analyte in the mobile phase, this value being much larger than the coefficient of diffusion in the stationary phase.

Fig. 5 depicts the measurements of the amplitude $|\kappa|$ of the optical signal versus time for an injection of cyclopentane. The retention ratio p was 0.077 as measured by standard chromatography. Fitting the data with Eqs. (7) and (8), taking $\Delta\beta = 1.61\ \mathrm{cm}^{-1}$, one calculates a diffusion coefficient of $0.030\ \mathrm{cm}^2/\mathrm{s}$ for pentane in helium, while the value reported in the literature is $0.092\ \mathrm{cm}^2/\mathrm{s}$ [17]. The difference may be explained by the approximation of the vapor zone by a Gaussian, which actually is far from being the case, as shown in the inset of Fig. 5. In any case, we think that obtaining an evaluation of the diffusion coefficient in the same order of magnitude as the one found in the literature using our optical sensor is worth noting. Through calibration and control of the injection, one can anticipate that a significant improvement might be achieved.

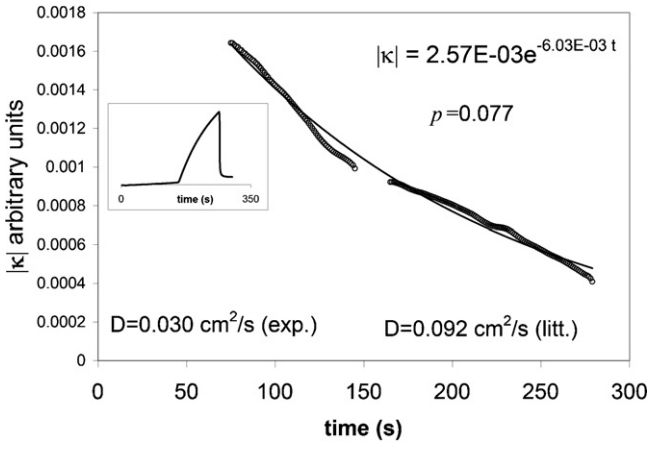

Fig. 5. Evaluation of the diffusion coefficient of cyclopentane in helium at 30 °C fromt the plot of $|\kappa|$ according to time. The insert shows the corresponding (asymmetric) eluted peak.

5. Description of the envelope of the optical signal

In Fig. 1, the variation of the baseline of the optical signal is designated by the circle A. The presence of this envelope has been reported previously [1], but its explanation was postponed. In what follows, a physical explanation for the origin of this signal envelope is provided and its implication discussed.

5.1. Equations for the envelope

In the model discussed in Section 3 (referring to circle B in Fig. 1) only a rotation of the birefringence axis is attributed to the absorption of the analyte in the stationary phase. The value of the birefringence of the waveguide itself is assumed to be constant during the passage of an analyte. This is not exactly the case and the apparition of an envelope in the signal is a consequence of a variation of the fiber's birefringence caused by the absorption of the analyte. (In other words, this absorption alters differently effective refractive indices n_x and n_y.) Moreover, this envelope would not appear if the angle of injection of polarized light was perfectly aligned with one of the polarization axes of the capillary optical fiber.

To describe the optical signal's envelope, the simple model of a tilted birefringent plate placed between two polarizers is sufficient. Using the Jones matrix formalism [11] and ignoring mode coupling, one can obtain the following equation that describes the light transmission of the waveguide *only for the envelope*:

$$T = \sin^2(\theta_i)\sin^4(\theta_a) + \cos^2(\theta_i)\cos^4(\theta_a) + \cos^2(\theta_a)\sin^2(\theta_a) + \frac{\sin(2\theta_i)\sin(2\theta_a)}{2}\cos(\Phi(t)), \tag{9}$$

where θ_i is the angle of the polarizer and is equivalent to the injection angle at the input of the birefringent plate, θ_a is the angle of the output polarizer, and $\Phi(t)$ is the phase shift caused by the change in birefringence ΔB. We consider that the change of birefringence is proportional to the amount of analyte absorbed into the stationary phase, namely:

$$\Delta B(z) = K\,C(z), \tag{10}$$

where K is a constant of proportionality. The phase $\Phi(t)$ does not depend on the distribution of the analyte, but to its total amount thereof. It is given by:

$$\Phi(t) = \frac{2\pi}{\lambda}\left(BL - \int_0^L \Delta B(z,t)dz\right), \tag{11}$$

B being the birefringence of the empty capillary fiber.

The first term on the right side of Eq. (11) is a constant and the variation of the envelope is solely due to the term under the integral. Eq. (9) suggests that the envelope will depend on the injection angle θ_i, but this is not controllable with the current configuration of the sensor. It also depends on the angle of the analyzer θ_a which can be changed.

Fig. 6 shows the change of the sign of the envelope for different angles of the output polarizer.

By inspection of Eq. (11), it can also be predicted that the envelope will depend on the wavelength of the light source. This is demonstrated in Fig. 7 for a same amount of analyte but for measurements performed at different wavelengths. By properly selecting the wavelength, the envelope can be made positive, negative or cancelled. Eq. (11) predicts that the evolution of the envelope will oscillate according to wavelength and this is demonstrated by

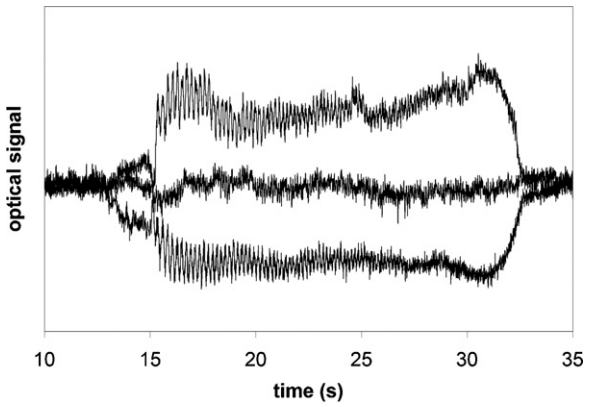

Fig. 6. Demonstration that the envelope can be made positive, negative or suppressed by rotating the analyzer.

the fact that it can be cancelled at both 1550 and 1640 nm. A more precise experiment should make it possible to measure the dependence of the birefringence of the capillary fiber according to the quantity of analyte injected.

5.2. Effect of excessive amount of analyte in the capillary fiber

Finally, Eqs. (11) and (9) imply that the height of the envelope will depend linearly on the total amount of analyte in the capillary only for small quantities. For higher quantities, the envelope's height should reverse when Φ takes values above π. This is indeed the case, as shown in Fig. 8 where the theoretical calculations and experimental measurements show the same signal pattern.

6. Discussion

The most important information from this study on the quantitative aspect of the polarimetric migration rate sensor is that the strength of polarization modes coupling, as measured by the height of a velocity peak, is related to the spatial derivative (gradient) of the vapor zone distribution. This is very important because it means that for an equal amount of injected analyte, the height of the velocity peak can be different. For example this height can be very large if the vapor zone has a steep front and/or tail, but smaller, or even zero, if the vapor zone is spatially extended in the capillary. One consequence is that the amplitude of oscillation decreases with time following the dispersion of the vapor zone. However, as the solution of the differential equations that govern a chromatographic process ([14], p. 49, [16], p. 26) is unique when initial conditions are the same, this means that for a same shape of the vapor zone at the injection, the vapor zone distribution is the same when the vapor moves along the capillary. Consequently, the sole necessary condition for proper quantification with the velocity sensor is reproducible injections.

First estimates have shown that the sensor is less sensitive than the TCD which was used. Certainly there is room for improving sensor's sensitivity. First at the instrumental level, the working wavelength can be optimized and the losses of the optical connections can be reduced so as to improve the S/N ratio of the power meter which is used to measure the sensor light transmission. Moreover, the theory predicts that a reduction of the injection peak width, which will create steep slopes dC/dz, would increase the oscillation amplitude. Secondly, the capillary fiber itself could be improved by fine tuning the angle between the optical axes of the waveguide and the capillary for a particular refractive index of the stationary phase. Also, it has been shown that the evanescent

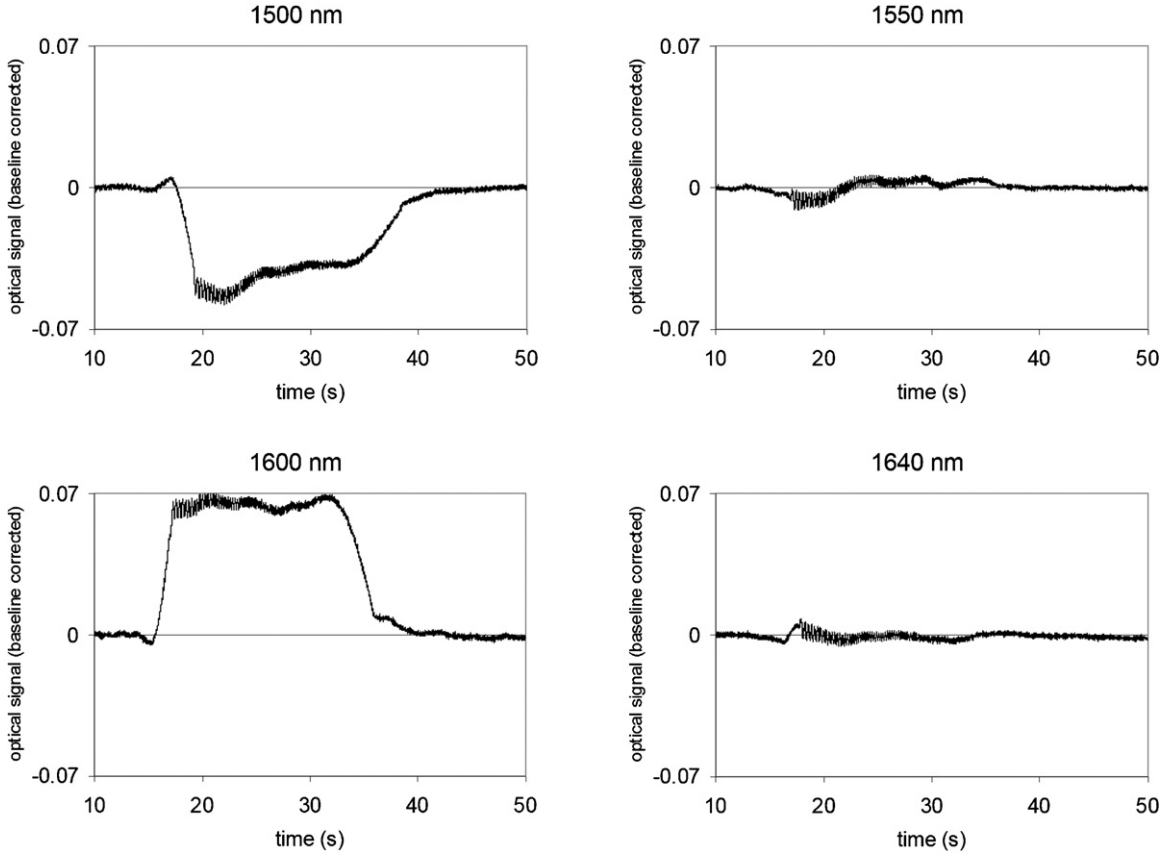

Fig. 7. Effects of wavelength on the signal envelope. The wavelengths were selected to maximize, minimize and cancel the envelope.

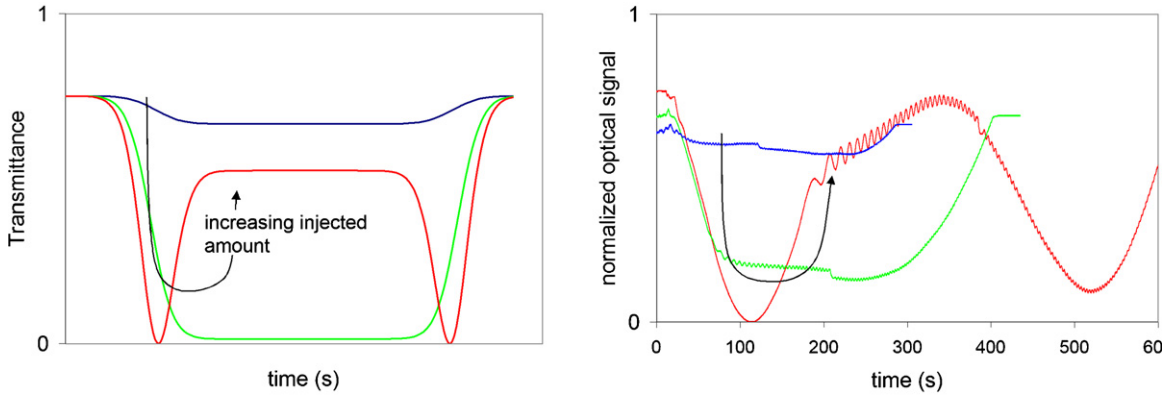

Fig. 8. Effect of analyte quantity on the signal envelope. Left: theory; right: experiment. When the quantity is large enough, the phase shift becomes larger than π and the effect on envelope strength reverses.

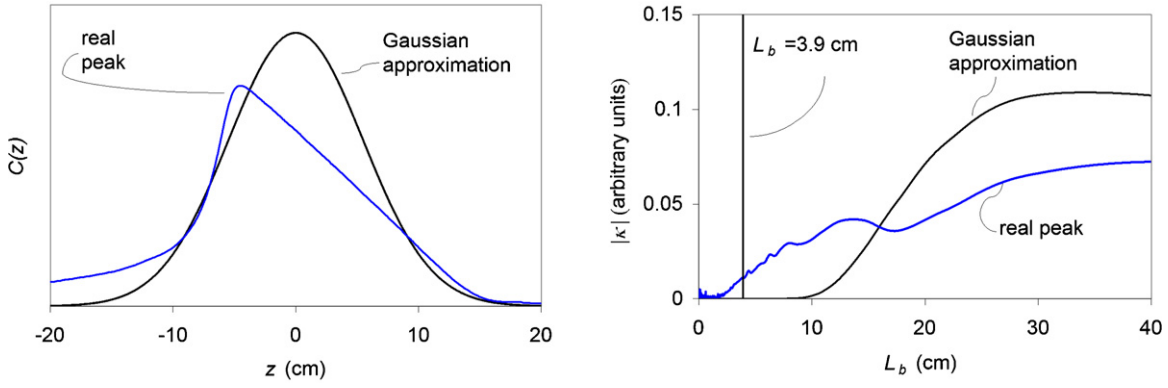

Fig. 9. Effect of the peak shape on the sensor sensitivity. Left: peak shapes; right: sensitivity curves. The peak full width is around 22 cm. This figure demonstrates that the sensor is more sensitive to an asymmetric peak having a steep edge than a smooth one having the same width.

wave extends a few microns into the capillary [7]. By increasing the thickness of the stationary phase (for the present experiments it was 0.5 μm), this evanescent wave will interact with more material, thus increasing the mode coupling strength. At first glance, as long as the stationary phase is thinner than the evanescent wave extent, one can expect that the sensitivity will be proportional to its thickness. Finally, it is worth noting that, since the amount of analyte necessary to produce a given change in refractive index in the stationary phase is inversely proportional to the square of the capillary radius, the sensitivity in mass will be higher for smaller capillaries.

With the injector we were using, the vapor zone extended over a few tens of centimeters. A question is then, why is the sensor sensitive if the peaks extend over a length which exceeds significantly the polarization beat length of the waveguide? The answer is: because the peaks are not Gaussian, so most of the polarization mode coupling comes from the sharp edges of real peaks. This can be understood with the following numerical example. Here, the spatial shape of the vapor zone is assumed to be the same as the shape of the elution peak. Fig. 9 depicts the assumed shape of a real peak (heptane) and an equivalent Gaussian peak, both having approximately the same width and the same surface. Their Fourier transforms, on the right of the figure (from Eqs. (2) and (5)), give the numerical function describing the amplitude $|\kappa|$ of a velocity peak for the vapor zone width of 22 cm. The beat length L_b of the capillary fiber was 3.9 cm, so the numerical function of Fig. 9 gives a value of $|\kappa| = 6.2 \times 10^{-5}$ for the Gaussian peak and $|\kappa| = 1.1 \times 10^{-2}$ for the real one. Consequently, the real peak causes an amplitude of oscillation which is 175 times higher than for an equivalent Gaussian one. This calculation is a good demonstration that a proper peak modulation at the injection can have a significant effect on the sensitivity of the optical sensor. Certainly the peak presented in Fig. 5 does not have an acceptable shape for chromatography but, since a less overloaded column should give two steep edges rather than one, one can expect that typical GC peaks will have a positive effect on sensor's sensitivity even if smaller quantities are injected.

7. Conclusion

In this paper, we have presented the equation that relates the height of a velocity peak measured by a fiber optic migration rate sensor to the vapor zone distribution in capillary gas chromatography. Experiments corroborated this model. The height of a velocity peak is proportional to the amount of analyte in the capillary and also depends on the vapor zone distribution. The sensitivity is related to the spatial gradient of the vapor zone. Consequently, the sensor is more sensitive to vapor zones having steep edges than to vapor zones having slowly varying ones. As the response of the sensor is linear relative to a thermal conductivity detector, its use for quantitative analysis is surely feasible. Knowing now the relation between analyte quantity and optical signal modulation, future work will have to focus on the determination of mixtures composition and on the number of analytes it can resolve. However, to achieve this goal, one must fisrt develop a more rugged sensor version that can withstand the high temperature encountered in normal GC applications.

Certainly, there are still plenty of studies to be done on the migration rate sensor. From the standpoint of sensitivity improvement, such work will mainly be a technical challenge, but from the

theoretical point of view, the resolution of velocity peaks remains to be studied. If all these issues can be solved, we think the sensor could be applied, for instance, to study physicochemical phenomena inside the column, to detect and study stationary phases' defects, or to adjust and optimize chromatograph parameters in real-time, during the separation process.

Acknowledgments

The authors whish to thank Nathalie Bornais, Steeve Morency and Huimin Zheng for the making of the optical fiber. They are also grateful to André Fougères for helpful discussion.

Parts of this work were presented at the 34th International Symposium on Capillary Chromatography held in Riva del Garda, Italy on June 1–4 2010.

Appendix A.

The amount C of pentane detected by the optical sensor has been calculated by the following least squares equation:

$$C = (M^T M)^{-1} M^T S, \tag{12}$$

where M is the vector containing the numerical values of the exponential fit. The product $(M^T M)^{-1} M^T$ is the left pseudo-inverse of M. S is the un-normalized data vector containing the values $|\kappa|$ according to time.

References

[1] S. Caron, C. Paré, P. Paradis, H. Zheng, A. Proulx, A. Fougères, J Chromatogr. A 1217 (2010) 3435.
[2] J. Liu, Y. Sun, D.J. Howard, G. Frye-Mason, A.K. Thompson, S. Ja, S.K. Wang, M. Bai, H. Taub, M. Almasri, X. Fan, Anal. Chem. 82 (2010) 4370.
[3] S.I. Shopova, I.M. White, Y. Sun, H. Zhu, X. Fan, G. Frye-Mason, A. Thompson, S.-J. Ja, Anal. Chem. 80 (2008) 2232.
[4] R.E. Synovec, A.W. Sulya, L.W. Burgess, M.D. Foster, C.A. Bruckner, Anal. Chem. 67 (1995) 473.
[5] C.A. Bruckner, R.E. Synovec, Talanta 43 (1996) 901.
[6] S. Caron, J.M. Trudeau, P. Paradis, C. Paré, B. Bourliaguet, C. Meneghini, 17th International Conference on Optical Fibre Sensors, Bruges, Belgium, SPIE 5855, 2005, p. 575.
[7] S. Caron, C. Paré, P. Paradis, J.M. Trudeau, A. Fougères, Meas. Sci. Technol. 17 (2006) 1075.
[8] S. Caron, C. Paré, P. Paradis, A. Fougères, 18th International Conference on Optical Fibre Sensors, Cancún, Mexico, 2006, Paper ThB5.
[9] S. Caron, C. Paré, B. Bourliaguet, United States Patent 7403673 (2008).
[10] S. Caron, C. Paré, A. Proulx, P. Grenier, V. Matejec, Photonics North 2009, Québec, Canada, SPIE Vol. 7386, 2009, p. 73861E.
[11] F.L. Pedrotti, L.S. Pedrotti, Introduction to Optics, Prentice-Hall Inc., Englewood Cliffs, NJ, 1987, chapter 17.
[12] Accepted for Presentation at the 21st International Conference on Optical Fiber Sensors, OFS-21, Ottawa, Canada, May 15–19, 2011, paper 7753-180.
[13] R.N. Bracewell, The Fourier Transform and its Applications, 2nd ed., McGraw-Hill, New York, 1978.
[14] J.Å. Jönsson (Ed.), Chromatographic Theory and Basic Principles, Marcel Dekker, New York, 1987.
[15] K.R. Beebe, R.J. Pell, M.B. Seasholtz, Chemometrics: A Practical Guide, John Wiley & Sons, New York, 1998.
[16] J.C. Giddings, Dynamics of Chromatography: Principles and Theory, Marcel Dekker, New York, 1965.
[17] R.W. Elliott, H. Watts, Can. J. Chem. 50 (1972) 31.